Parametric excitation of eigenmodes in microscopic magnetic dots

Henning Ulrichs, Vladislav E. Demidov, Sergej O. Demokritov, and Sergei Urazhdin

Phys. Rev. B **84**, 094401 — Published 2 September 2011

DOI: 10.1103/PhysRevB.84.094401

Parametric excitation of eigenmodes in microscopic magnetic dots

Henning Ulrichs*, Vladislav E. Demidov, and Sergej O. Demokritov

Institute for Applied Physics and Center for Nonlinear Science, University of Muenster, Corrensstrasse 2-4, 48149 Muenster, Germany

Sergei Urazhdin

Department of Physics, West Virginia University, Morgantown, WV 26506, USA

We utilize time- and space-resolved Brillouin light scattering spectroscopy to study the parametric excitation of spin-wave eigenmodes in microscopic Permalloy dots. We show that the fundamental center eigenmode has the smallest excitation threshold. With the increase of the pumping power above this threshold, higher-order dipole-dominated eigenmodes with both even and odd spatial symmetry also become excited. At microwave power levels far above the threshold, the multimode excitation regime is suppressed due to the parametric excitation of short-wavelength exchange-dominated spin-wave modes. Our results provide important insight into the physics of parametric processes in microscopic magnetic systems.

PACS numbers: 75.40.Gb, 85.75.-d, 75.30.Ds, 75.75.-c

* Corresponding author, e-mail: henning.ulrichs@uni-muenster.de

I. INTRODUCTION

Parametric processes in magnetic systems were observed by Bloembergen and Damon[1] and theoretically explained by Anderson and Suhl[2] more than fifty years ago. Since then, they have been intensively studied in the context of applied physics as well as basic research.[3-15] Parametric processes can be utilized for amplification and manipulation of spin-wave pulses,[7-9] parametric stimulation and recovery of microwave signals,[10] and wave-front reversal.[11] They also can be used as a powerful experimental tool in studies of spin-wave solitons and two-dimensional bullets,[7,8,12,13] as well as magnon Bose-Einstein condensates.[14,15]

One of the main parameters governing the efficiency of parametric excitation is the dynamic damping.[16] Monocrystalline yittrium iron garnet (YIG) films are characterized by extremely low magnetic damping (Gilbert damping parameter $\alpha<10^{-4}$), and thus have become the material of choice for the studies of parametric excitation and amplification of magnetization oscillations and waves. As a consequence of the low damping in YIG, moderate microwave pumping levels are sufficient for the parametric excitation, enabling studies of strongly nonequilibrium states such as parametrically driven magnon gas in strongly nonlinear regime.[17]

As a material for technical applications, YIG has several drawbacks. High-quality YIG films can be grown only on special substrates such as gallium gadolinium garnet, which makes the fabrication process incompatible with conventional silicon-based semiconductor technology. Additionally, this material is difficult to structure and it also exhibits a strong dependence of the magnetic properties on temperature due to the relatively low Curie point. In contrast, polycrystalline transition metal ferromagnetic films can be easily grown by sputtering or evaporation on a variety of substrates

including silicon, and structured on sub-micrometer scale by standard lithography techniques. Among these materials, $Ni_{80}Fe_{20}$=Permalloy (Py) is most widely used for basic research and applied studies due its low crystalline anisotropy and small damping ($\alpha<10^{-2}$). Py has been utilized as a working medium in spin-torque nano-oscillators,[18-21] magnonic crystals,[22-26] domain wall motion-based memory devices,[27] and spin-wave logic circuits.[28]

Magnetic damping in Py is relatively small compared to other metallic ferromagnets, but is still much larger than in YIG, resulting in a significantly higher threshold power required for parametric excitation. For instance, parametric excitation of spin waves in Permalloy films has been achieved only with microwave power levels of at least a few Watts.[29,30] This problem can be overcome by reducing the dimensions of the magnetic samples to nanometer scale and concentrating the pumping energy into a smaller volume, thus producing with moderate driving power a large local microwave field sufficient for parametric excitation.[31,32]

In this article, we report an experimental investigation of the parametric excitation of spin-wave modes in an elliptical Py dot with submicrometer dimensions fabricated on top of a microscopic microwave transmission line. To analyze the spectral and spatial characteristics of the excited modes, we utilized time- and space-resolved micro-focus Brillouin light scattering (BLS) spectroscopy.[33] The parametric excitation threshold power of about 1 mW was significantly smaller than in the extended Py films, enabling us to investigate parametric excitation processes far above the threshold. We show that above the threshold, many different dipole-dominated eigenmodes are excited simultaneously. At large parametric pumping power, short-wavelength exchange-dominated spin-wave modes also become excited. The transfer of the parametric

pumping energy into the short-wavelength part of the mode spectrum results in a decreased excitation efficiency of the dipole-dominated modes. This redistribution of energy does not significantly affect the excitation of the lowest-frequency modes of the dot. Consequently, the fundamental center and the edge modes can be efficiently excited by the parametric pumping both at small and at large pumping power levels. These results are important for the development of integrated magnetic devices utilizing parametric processes for excitation and amplification of magnetization oscillations.

II. SAMPLE AND MEASUREMENT SETUP

Figure 1 shows a scanning electron micrograph of the studied sample, which consists of a 10 nm thick Py film patterned by electron-beam lithography and ion milling into an elliptical dot with lateral dimensions of 1000 by 500 nm. The dot is fabricated directly on top of a 1 μm wide and 160 nm thick Au microstrip transmission line. A dc magnetic field H=400-700 Oe was applied along the short axis of the Py ellipse. The data presented below were obtained at H=700 Oe. To excite the magnetization dynamics, microwave pulses with duration of 100 ns and a repetition period of 2 μs were applied to the transmission line. The pulse power was varied between 0.1 mW and 50 mW. The microwave pulses created a dynamic magnetic field **h** parallel to the direction of the static magnetization.

The detection of the magnetization dynamics was performed by micro-focus BLS technique described in detail in Ref. 33. This technique combines the spectral and the temporal resolution of the conventional BLS[34] with diffraction-limited spatial resolution of about 250 nm determined by the size of the probing laser spot. The intensity of the

scattered light at a given frequency is proportional to the square of the dynamic magnetization amplitude at this frequency, at the position of the probing spot.

The dynamic magnetic field **h** was parallel to the static magnetization in our experimental geometry. In this configuration, the microwave field cannot linearly excite magnetization dynamics, since the corresponding component of the dynamic magnetic susceptibility tensor is equal to zero[16]. Instead, the dynamics can be excited by a higher-order parametric excitation process[35]. In the quasiparticle picture, this process can be understood as splitting of a microwave photon with frequency f_P and wave vector $k_P \approx 0$ into two magnons with frequency $f_P/2$ and wave vectors that are equal in magnitude and opposite in direction[16]. In accordance with this picture, in our experiments we detected magnetization oscillations at half of the applied microwave pumping frequency f_P.

In confined sample geometries, quantization of the spin-wave spectrum imposes limitations on the parametric excitation. Specifically, the dynamic magnetization response exhibits resonant spectral behavior, with resonant frequencies equal to those of the system's eigenmodes. By utilizing the spectral sensitivity of the BLS technique to detect only the dynamic signal at the frequency of a particular mode, one can selectively map out its spatial profile. Additionally, by synchronizing the microwave pulses with the spectrometer clock, the time dependence of the magnetization response to the excitation pulses can be recorded with resolution of 1 ns.

III. EXPERIMENTAL RESULTS AND ANALYSIS

III.a. Spectral characteristics of parametric excitation

Figure 2 shows the BLS spectra recorded at different values of the microwave pumping power P between 1 and 50 mW, providing a survey of the spectroscopic properties and power-dependent dynamical regimes of the system. To record the spectra, the laser spot was positioned at the center of the Py dot. The pumping frequency f_P was varied between 8 and 20 GHz and the BLS intensity was simultaneously measured at $f_P/2$.

Because of the threshold nature of the parametric excitation, no dynamic magnetization was detected at $P<1$ mW. At $P=1$ mW, the spectrum exhibits a single peak at $f_0=7.1$ GHz ($f_p=14.2$ GHz) corresponding to the spin-wave eigenmode with the lowest parametric threshold [Fig. 2(a)]. At $P>2$ mW, a second peak appears at $f_2=8.5$ GHz, as illustrated in Fig. 2(b) for $P=2.5$ mW. At $P>3.2$ mW a third peak appears at $f_1=7.7$ GHz, as illustrated in Fig.2(c) for $P=5$ mW. Figures 2(b,c) demonstrate that all these peaks coexist. At even larger power levels, several additional peaks appeared in the spectra. For example, four closely spaced large peaks and an additional small peak at frequency f_e significantly below f_0 can be distinguished at $P=10$ mW [Fig 2(d)]. There is also a bump on the declining slope of the peak at f_0, suggesting that at least one additional mode with frequency close to f_0 may be excited.

This simple trend is reversed at excitation powers above 10 mW. The BLS spectra now exhibit only two peaks at frequencies f_0 and f_e [Fig. 2(e) and 2(f)]. These two peaks exhibit a nonlinear frequency shift with increasing P. In addition, they broaden and become noticeably asymmetric. The asymmetry is especially pronounced for the peak at f_0, which clearly has a significantly steeper rising slope than the declining slope, characteristic for a nonlinear resonance.[36-38]

III.b. Spatial characteristics of the parametrically excited modes

To identify the normal modes associated with the observed spectral peaks, we performed spatially resolved measurements at P=10 mW, where the largest number of peaks are observed. For each of the observed peaks, the excitation frequency was fixed at twice its central frequency, and two-dimensional mapping of the BLS intensity was performed. The probing spot was scanned in x- and y-directions with a step size of 50 nm across a 500 by 1000 nm rectangular area covering the Py dot. The left-side panels in Fig. 3 show pseudocolor-coded maps of the recorded BLS intensity. The right-side panels show one-dimensional cross sections of these maps along the major axis of the Py ellipse. It is important to note, that the measured two-dimensional maps and one-dimensional profiles represent a result of convolution of the local dynamic magnetization amplitude with the instrumental resolution function, resulting in a significant blurring of submicrometer spatial features.

Figure 3(a) shows that the mode at frequency f_0=7 GHz has a half-sine profile along the major axis, and does not exhibit any nodal lines. These characteristics indicate that it is the fundamental center mode of the Py dot.[39] The profile of the mode at frequency f_1=7.7 GHz [Fig. 3(b)] has two maxima on the long axis and a minimum at the center of the dot. This minimum is likely associated with the nodal line of the eigenmode. The BLS intensity does not vanish at the minimum, likely due to the limited spatial resolution of our technique.

The spatial profile of the mode at f_2=8.3 GHz [see Fig. 3(c)] has a maximum at the center, similar to the fundamental mode. In contrast to that mode, the profile is sharper near the maximum, and forms two broad shoulders with small bumps near the edges. As mentioned above, fine spatial features are blurred due to finite resolution of the setup.

Therefore, based on our data, the mode with the frequency f_2 can be interpreted as a mode with two nodal lines separating a central maximum from two side maxima located on the major axis of the Py ellipse.

The limitations of the spatial resolution of our technique prevented us from identifying the mode corresponding to the peak at f_3. This higher-order mode likely has three nodal lines. We also performed spatially resolved measurements at f_e=5.5 GHz, which revealed a typical spatial structure of the so-called edge mode, with maxima of the intensity close to the edges of the dot on the axis parallel to the direction of the static field, and a vanishing intensity at the center of the dot.

We note that the mode observed at f_1=7.7 GHz [Fig. 3(b)] is expected to have odd spatial symmetry, i.e. its dynamical amplitude profile is antisymmetric with respect to the minor axis of the dot. By symmetry, this mode cannot be directly excited by the usual linear excitation mechanism with a spatially uniform dynamic magnetic field. The symmetry of the mode at f_2 does not prohibit its linear excitation by a uniform field, but the excitation efficiency would be significantly smaller than for the fundamental mode at f_0.[40] In contrast, the efficiency of parametric excitation for all these modes is similar, as indicated by the similar amplitudes of the peaks in Fig. 2(d). Therefore, parametric excitation mechanism presents significant advantages compared to the linear excitation for the experimental studies of the eigenmode spectra in micro- and nano-magnets.

III.c. Dependence of the mode intensities on the pumping power.

We now analyze and interpret the dependences of the parametrically excited mode intensities on the pumping power. Figure 4 shows these dependences for the

fundamental mode (filled triangles), the higher-order mode at f_2 (open triangles), and the edge mode at f_e (circles). Both of the center modes exhibit similar non-monotonic behavior above their excitation thresholds: the intensities first increase, and then start to decrease with further increase of the pumping power. The intensity of the fundamental mode reaches a minimum at $P \approx 6$ mW and then increases again. In contrast, the BLS peak at f_2 becomes indistinguishable from the background at $P=12$ mW and does not recover at larger pumping powers. Similar behaviors were also observed for the higher-order modes at frequencies f_1 and f_3.

These data suggest the presence of a mechanism limiting the energy flow from the parametric pumping to the observed modes at large P. Although this mechanism influences all the observed modes, its effect on the higher-order modes is stronger than on the fundamental mode, leading to their complete suppression.

To interpret these behaviors, we recall that because of the intrinsic anisotropy of the magnetic eigenmode spectrum, the frequencies of the modes only weakly depend on the number of nodal lines perpendicular to the magnetization.[41] As a consequence, for each mode with nodal lines parallel to the static magnetization [see Fig. 3], there are, generally speaking, many nearly degenerate modes with a finite number of nodal lines perpendicular to the magnetization. For example, at frequencies f_1-f_3 there are a number of exchange-dominated modes with very short effective wavelengths in the direction parallel to the magnetization. These modes cannot be detected by the BLS technique, which is sensitive predominantly to the long-wavelength modes.

The exchange-dominated modes are generally characterized by stronger damping and weaker coupling to the pumping field, and consequently have a larger excitation

threshold compared to the dipole-dominated modes[41]. Therefore, only the dipole-dominated modes are excited at small P, and in this regime their intensity increases with P. As P reaches the threshold value for the excitation of the exchange-dominated modes, additional scattering channels become effective that redistribute the energy among the modes. While the details of these processes are presently unknown, one can generally expect that the increase in the amplitudes of exchange-dominated magnetization oscillations results in a nonlinear scattering of the dipole-dominated oscillations into the short-wavelength part of the mode spectrum, creating additional nonlinear damping channels for the dipole-dominated modes. As a result, the flow of the energy from the pumping to the dipole-dominated modes decreases leading to a decrease of their intensity and, at sufficiently large pumping power, to the complete suppression of the dipole-dominated modes.

This suppression mechanism is significantly less efficient for the fundamental mode, since it has the lowest frequency among the center modes, and consequently there are no exchange-dominated modes at the same frequency. Nevertheless, there are a number of modes with no nodal lines parallel to the magnetization and several nodal lines perpendicular to the magnetization whose frequency is only slightly different from that of the fundamental mode. The onset of their parametric excitation can be the origin of the decrease of the fundamental peak intensity at P>3 mW.

These modes are dipole-dominated and thus should be detectable by the BLS measurements. Indeed, the broadening of the fundamental peak at P>3 mW [compare Figs. 2(a) and 2(c)] and a bump on its declining slope [see Fig. 2(d)] can be interpreted as a signature of their excitation. In addition, in the interval P=3-8 mW spatially resolved measurements revealed deviations of the spatial profile of the mode at f_0 from

that shown in Fig. 3(a) for P=10 mW, which can be associated with simultaneous excitation of several dipole-dominated modes with different spatial profiles. The largest deviations were observed at P=6 mW corresponding to the minimum of the fundamental mode intensity. These deviations are dramatically reduced at P>10 mW. Based on these data one can conclude, that, in contrast to the competition between the dipole-dominated and exchange-dominated modes, the competition among the dipole-dominated modes results in the predominant energy flow into the fundamental mode of the dot at large P.

Finally, the intensity of the edge mode (circles in Fig. 4) increases monotonically with increasing P. This behavior is consistent with the intensity-suppression mechanisms discussed above: since the frequency of the edge mode lies far below the frequencies of all the other modes of the system, its intensity is not affected by their parametric excitation.

III.d. Temporal characteristics of the parametric excitation

In addition to the significance of parametric excitation as a spectroscopic tool, it can be used to determine other important dynamical parameters of the magnetic system. The time dependence of the excited mode amplitude at different pumping powers provides information about the magnetic damping constant, the strength of the microwave pumping field, and its coupling to the magnetic system (see Section IV for details).

We performed time-resolved measurements of the fundamental mode intensity at pumping powers between the threshold value of 1 mW and 50 mW, with temporal

resolution of 1 ns. Figures 5 (a) and 5(b) show time traces for P=1 mW and 3.2 mW, respectively. These data demonstrate that just above the parametric threshold the rate of intensity growth is small, but it quickly increases with increasing P.

Plotting the time-dependent intensity of the fundamental mode on the logarithmic scale, at P=1-4 mW we observe a well-defined initial exponential rise followed by saturation, as illustrated in Fig. 5(c) for P=3.2 mW. Fitting this exponential dependence, we obtain a characteristic rise time constant τ as a function of the pumping power for P<4 mW. At larger powers P>4 mW, the intensity growth becomes too abrupt to make a reliable estimate of τ, due to the limited temporal resolution of our measurement. Analysis given in Section IV suggests that the inverse of the time constant τ should depend linearly on h, which is proportional to the square root of the pumping power, $h = A\sqrt{P}$. Here, A is a calibration parameter determined by the sample geometry and the microwave losses in the transmission line. As expected, the experimentally determined values of $1/\tau$ follow a linear dependence on $\sqrt{P}$ [Fig. 5(d)].

IV. THEORY

Rigorous understanding of the nonlinear dynamical regimes in microscopic structures requires a self-consistent theory of parametric excitation taking into account the effects of the inhomogeneity of the internal demagnetizing field and the magnetization in the sample, as well as the boundary conditions governing spin-wave quantization. Nevertheless, the theory developed for extended magnetic films[41] can still be used to analyze the behavior of the studied system close to the threshold of the

parametric excitation. According to Ref. 41, the threshold amplitude of the dynamic magnetic field for the onset of the parametric excitation is given by

$$h_{th} = \omega_r / V , \qquad (1)$$

where $\omega_r = \alpha\omega$ is the relaxation frequency and $V = \gamma^2 4\pi M_s \left[P(k)\left(1+\sin^2(\varphi)\right) - 1 \right] / (4\omega)$ is a coefficient characterizing the coupling of the pumping field to the plane wave with frequency ω and wave vector **k** oriented in the film plane at an angle φ with respect to the direction of the static magnetization: $\varphi = \tan^{-1}(k_y/k_x)$. Here, $4\pi M_s$ is the saturation magnetization and $P(k) = 1 - \left(1 - \exp(-kd)\right)/kd$, where d is the film thickness.

To account for the finite lateral dimensions of the dot, we applied the standard spin-wave quantization scheme.[42] Within this approach, the fundamental center mode of the dot is approximated by a two-dimensional standing spin wave with the components of the wave vector $k_x = \pi/a$ and $k_y = \pi/b$, where a=1000 nm and b=500 nm are the lateral sizes of the dot in x and y directions, respectively. In this approximation, the coupling coefficient is $V = 1.63 \cdot 10^7$ (Oe·s)$^{-1}$.

Above the threshold, the amplitude of the parametrically excited mode is expected to grow exponentially with a characteristic time constant (see Ch.5.3 in Ref. 43)

$$\tau = 1 / \left(hV - \omega_r \right) . \qquad (2)$$

In agreement with this result, the experimental values for $1/\tau$ scale linearly with h [Fig. 5(d)]. As follows from Eq. (2), $1/\tau$ is equal to the relaxation frequency ω_r at h=0 and vanishes at $h=h_{th}$. Fitting the experimental data of Fig. 5(d) with a linear function and extrapolating to P=0, we obtain $\omega_r = 0.36 \cdot 10^9$ s^{-1} corresponding to the Gilbert damping parameter α=0.008, in excellent agreement with the known value for Py[44]. From the

same fit we also obtain the threshold power P_{th}=0.6 mW corresponding to the exact compensation of the magnetic relaxation by the parametric pumping. Finally, from the slope of the linear dependence, we obtain the calibration factor A=29 Oe/(mW)$^{1/2}$. This value is in a reasonable agreement with the estimate A=24 Oe/(mW)$^{1/2}$ based on the nominal geometrical parameters of the microstrip line.

V. CONCLUSIONS

In conclusion, we have demonstrated parametric excitation of spin-wave modes in microscopic magnetic-film structures at moderate microwave powers. Parametric processes can be utilized for studies of the eigenmode spectra and other dynamical characteristics in micro- and nano-magnets. The low threshold power for parametric excitation in microscopic systems enables observation of complex nonlinear phenomena such as mode competition and nonlinear parametric resonance. Moreover, the low threshold power makes parametric processes in microscopic structures useful for technical applications such as parametric amplification of spin waves in integrated magnonic devices.

ACKNOWLEDGEMENTS

We acknowledge support from Deutsche Forschungsgemeinschaft, the European Project Master (No. NMP-FP7 212257), the NSF grants DMR-0747609 and ECCS-0967195, and the Research Corporation.

REFERENCES

[1] N. Bloembergen and R.W. Damon, Phys. Rev. **85**, 699 (1952).

[2] P.W. Anderson and H. Suhl, Phys. Rev. **100**, 1788 (1955).

[3] V. E. Zakharov, V. S. Lvov, and S. S. Starobinets, Sov. Phys. JETP **32**, 656 (1971).

[4] V. N. Venitskii, V. V. Eremenko, E. V. Matyushkin, Sov. Phys. JETP **50**, 934 (1979).

[5] W. Wettling, W. D. Wilber, P. Kabos, and C. E. Patton, Phys. Rev. Lett. **51**, 1680 (1983).

[6] P. Kabos, C. E. Patton, G. Wiese, A. D. Sullins, E. S. Wright, and L. Chen, J. Appl. Phys. **80**, 3962 (1996).

[7] A. V. Bagada, G. A. Melkov, A. A. Serga, and A. N. Slavin, Phys. Rev. Lett. **79**, 2137 (1997).

[8] P. A. Kolodin, P. Kabos, C. E. Patton, B. A. Kalinikos, N. G. Kovshikov, and M. P. Kostylev, Phys. Rev. Lett. **80**, 1976 (1998).

[9] K. R. Smith, V. I. Vasyuchka, M. Wu, G. A. Melkov, and C. E. Patton, Phys. Rev. B **76**, 054412 (2007).

[10] A. A. Serga, A. V. Chumak, A. André, G. A. Melkov, A. N. Slavin, S. O. Demokritov, and B. Hillebrands, Phys. Rev. Lett. **99**, 227202 (2007).

[11] A. L. Gordon, G. A. Melkov, A. A. Serga, A. N. Slavin, V. S. Tiberkevich, A. V. Bagada, JETP Lett. **67**, 913 (1998).

[12] S. O. Demokritov, A. A. Serga, V. E. Demidov, B. Hillebrands, M. P. Kostylev, and B. A. Kalinikos, Nature **426**, 159 (2003).

[13] A. A. Serga, B. Hillebrands, S. O. Demokritov, A. N. Slavin, P. Wierzbicki, V. Vasyuchka, O. Dzyapko, and A. Chumak, Phys. Rev. Lett. **94,** 167202 (2005).

[14] S. O. Demokritov, V. E. Demidov, O. Dzyapko, G. A. Melkov, A. A. Serga, B. Hillebrands, and A. N. Slavin, Nature **443**, 430 (2006).

[15] V. E. Demidov, O. Dzyapko, M. Buchmeier, T. Stockhoff, G. Schmitz, G. A. Melkov, and S. O. Demokritov, Phys. Rev. Lett. **101**, 257201 (2008).

[16] A. G. Gurevich and G. A. Melkov, *Magnetization Oscillation and Waves* (CRC Press, Boca Raton, 1996).

[17] V. E. Demidov, O. Dzyapko, S. O. Demokritov, G. A. Melkov, and A. N. Slavin, Phys. Rev. Lett. **99**, 037205 (2007).

[18] I. N. Krivorotov, N. C. Emley, J. C. Sankey, S. I. Kiselev, D. C. Ralph, and R. A. Buhrman, Science **307**, 228 (2005).

[19] F. B. Mancoff, N. D. Rizzo, B. N. Engel, and S. Tehrani, Nature **437**, 393 (2005).

[20] M. R. Pufall, W. H. Rippard, and S. E. Russek, S. Kaka, J. A. Katine, Phys. Rev. Lett. **97,** 087206 (2006).

[21] V.E. Demidov, S. Urazhdin, and S.O. Demokritov, Nature Materials **9**, 984 (2010).

[22] S. Neusser and D. Grundler, Adv. Mat. **21**, 2927 (2009).

[23] V. V. Kruglyak, P. S. Keatley, A. Neudert, R. J. Hicken, J. R. Childress, and J. A. Katine, Phys. Rev. Lett. **104**, 027201 (2010).

[24] S. Tacchi, M. Madami, G. Gubbiotti, G. Carlotti, H. Tanigawa, T. Ono, and M. P. Kostylev, Phys. Rev. B **82**, 024401 (2010).

[25] A. V. Chumak, P. Pirro, A. A. Serga, M. P. Kostylev, R. L. Stamps, H. Schultheiss, K. Vogt, S. J. Hermsdoerfer, B. Laegel, P. A. Beck, and B. Hillebrands, Appl. Phys. Lett. **95**, 262508 (2009).

[26] Z. K. Wang, V. L. Zhang, H. S. Lim, S. C. Ng, M. H. Kuok, S. Jain, and A. O. Adeyeye, Appl. Phys. Lett. **94**, 083112 (2009).

[27] S. S. P. Parkin, M. Hayashi, and L. Thomas, Science **320**, 5873 (2008).

[28] A. Khitun, M. Bao, and K. L. Wang, J. Phys. D: Appl. Phys. **43**, 264005 (2010).

[29] S. Y. An, P. Krivosik, M. A. Kramer, H. M. Olson, A. V. Nazarov, and C. E. Patton, J. Appl. Phys. **96**, 1572 (2004).

[30] G. A. Melkov, Yu. V. Koblyanskiy, R. A. Slipets, A. V. Talalaevskij, and A. N. Slavin, Phys. Rev. B **79**, 134411 (2009).

[31] V. E. Demidov, H. Ulrichs, S. O. Demokritov, and S. Urazhdin, Phys. Rev. B **83**, 020404(R) (2011).

[32] S. Urazhdin, V. S. Tiberkevich, and A.N. Slavin, Phys. Rev. Lett. **105**, 237204 (2010).

[33] S. O. Demokritov and V. E. Demidov, IEEE Trans. Magn. **44**, 6 (2008).

[34] S. O. Demokritov, B. Hillebrands, and A. N. Slavin, Phys. Rep. **348**, 441 (2001).

[35] E. Schlömann, J. J. Green, and U. Milano, J. Appl. Phys. **31**, S386 (1960).

[36] T. Gerrits, P. Krivosik, M. L. Schneider, C. E. Patton, and T. J. Silva, Phys. Rev. Lett. **98,** 207602 (2007).

[37] Y. S. Gui, A. Wirthmann, and C.-M. Hu, Phys. Rev. B **80**, 184422 (2009).

[38] Y. Khivintsev, B. Kuanr, T. J. Fal, M. Haftel, R. E. Camley, Z. Celinski, and D. L. Mills, Phys. Rev. B **81**, 054436 (2010).

[39] I. Neudecker, K. Perzlmaier, F. Hoffmann, G. Woltersdorf, M. Buess, D. Weiss, and C. H. Back, Phys. Rev. B **73**, 134426 (2006).

[40] V. E. Demidov, M. P. Kostylev, K. Rott, P. Krzysteczko, G. Reiss, and S. O. Demokritov, Appl. Phys. Lett. **95**, 112509 (2009).

[41] D. N. Chartoryzhskii, B. A. Kalinikos, and O. G. Vendik, Solid State Commun **20**, 985 (1976).

[42] K. Yu. Guslienko, S. O. Demokritov, B. Hillebrands, A. N. Slavin Phys. Rev. B **66**, 132402 (2002).

[43] V. S. L'vov, *Wave Turbulence under Parametric Excitation* (Springer-Verlag, Berlin-Heidelberg, 1994).

[44] J. O. Rantschler, R. D. McMichael, A. Castillo, A. J. Shapiro, W. F. Egelhoff, Jr., B. B. Maranville, D. Pulugurtha, A. P. Chen, and L. M. Connors, J. Appl. Phys **101**, 033911 (2007).

Figure captions

Fig. 1. (Color online) Scanning electron micrograph of the sample.

Fig. 2. BLS spectra recorded at powers of the parametric pumping varying from 1 to 50 mW, as labeled. Horizontal axis corresponds to half of the pumping frequency.

Fig. 3. (Color online) Left: pseudocolor-coded maps of the BLS intensity. Right: one-dimensional cross sections of the maps along the major axis of the Py ellipse, as marked by the dashed lines. Panels (a)-(c) are acquired at the labeled frequency values corresponding to three different spectral peaks.

Fig. 4. (Color online) Dependence of the BLS peak intensity on the pumping power for the fundamental mode at f_0 (filled triangles), for the higher-order mode at f_2 (open triangles), and for the edge mode at f_e (open circles).

Fig. 5. (Color online) (a) and (b) Time traces of the fundamental mode intensity at the labeled values of the pumping power. t=0 corresponds to the start of the pumping pulse. (c) Time dependence of intensity on the logarithmic scale at P=3.2 mW. Line shows the result of a fit by an exponential function. (d) The inverse of amplitude rise time constant vs $\sqrt{P} \propto h$. Line is the best linear fit of the data.

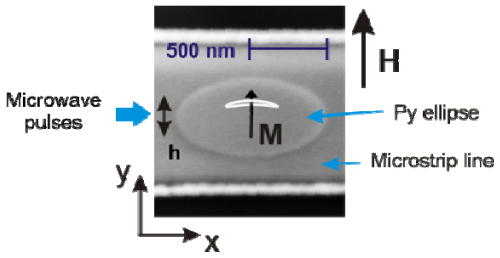

Fig. 1

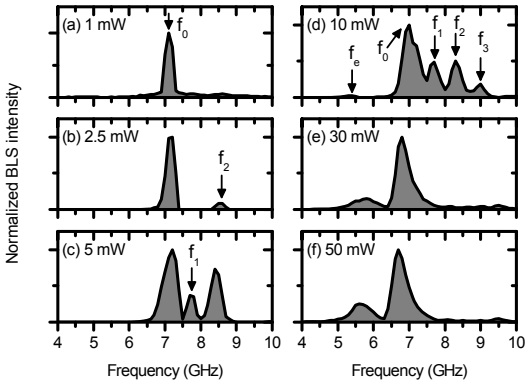

Fig. 2

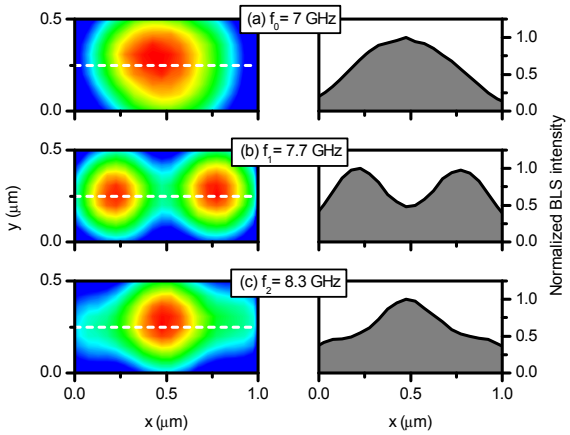

Fig. 3

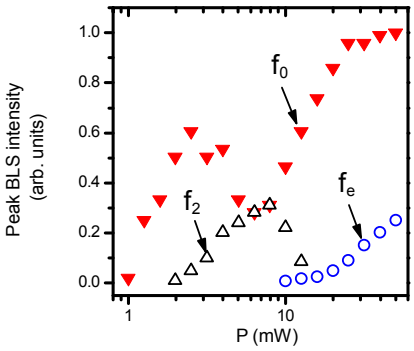

Fig. 4

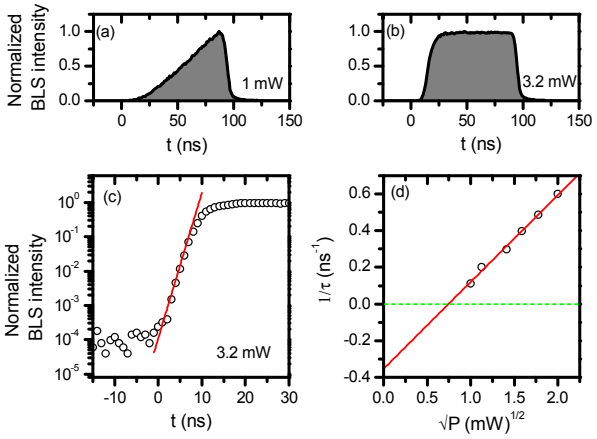

Fig. 5